Bleomycin Loaded Magnetic Chitosan Nanoparticles as Multifunctional Nanocarriers

DOĞA KAVAZ,[1] SEDAT ODABAŞ,[2] EYLEM GÜVEN,[3]
MURAT DEMİRBILEK[3] AND EMİR BAKİ DENKBAŞ[1,3,*]

[1]*Department of Chemistry, Hacettepe University Biochemistry Division, Beytepe, Ankara, Turkey*

[2]*Bioengineering Division, Hacettepe University, Beytepe, Ankara, Turkey*

[3]*Nanotechnology and Nanomedicine Division Hacettepe University, Beytepe, Ankara, Turkey*

ABSTRACT: Iron oxide (Fe_3O_4) containing magnetic chitosan nanoparticles were prepared with Concanavalin-A and Bleomycin as multifunctional nanocarriers for the targeted cancer therapy by co-precipitation techniques. The chemical structures of nanoparticles were analyzed by FTIR and the magnetic properties of the nanoparticles were evaluated by electron spin resonance technique and vibrational scanning mangnetometer measurements. The *in vitro* release profiles of Bleomycin were investigated and chitosan nanoparticles characteristics were optimized for subsequent *in vivo* applications. The magnetic chitosan nanoparticles are biocompatible-based MTT assays. The therapeutic potential of these nanoparticles are being investigated for *in vivo* applications.

KEY WORDS: iron-oxide nanoparticles, chitosan, magnetic nanoparticles, Bleomycin, Concanavalin-A.

INTRODUCTION

Cancer has become one of the leading causes of death, according to a new World Cancer Report from the International Agency for

*Author to whom correspondence should be addressed.
E-mail: denkbas@hacettepe.edu.tr
Figures 1 and 4 appear in color online: http://jbc.sagepub.com

0883-9115/10/03 0305–14 $10.00/0 DOI: 10.1177/0883911509360735

Research on Cancer [1]. Despite many conventional diagnosis and therapy techniques, such as radiological, physical, chemical, immunological, and surgical, many potential side-effects due to current treatment techniques on healthy tissue and organs exist [2–9]. To counter these cytotoxicity risks, several novel strategies were developed, such as chemotherapeutic pro-drugs activated at tumor site, tagged drugs, chemotherapy with immunotherapy, vascular targeting, interventional genetics, and magnetic drug guidance [10]. We investigated one of the most promising strategies, magnetic drug guidance, magnetic guided drug targeting, and magnetic responsive micro and nanocolloidal carriers in theragnosis of the cancer [11].

Magnetically guided drug delivery involves an external magnetic field to deliver nanoparticles to a desired target area where the medication is needed. The advantage being that the dosage of the medication can be reduced and the systemic effect of the drugs can be kept to a minimum level and localized [12]. Simultaneous application of an oscillating magnetic field increases the temperature of magnetic nanoparticles and used as hyperthermia therapy in oncology [13]. This form of treatment has received considerable attention because it could significantly reduce clinical side-effects compared to chemotherapy and radiotherapy. Iron oxide nanoparticles (Fe_3O_4) are magnetic and can be modified with biocompatible polymers to overcome aggregation and other problems related to iron oxide nanoparticles [14,15].

Chitosan, made from naturally occurring chitin, is a unique cationic polymer with gel- and film-forming properties. It is being investigated in the pharmaceutical industry for its potential in the development of drug delivery systems [16,17]. Chitosan has beneficial qualities, such as low toxicity, low immunogenicity, excellent biodegradability, biocompatibility as well as a high positive charge that easily forms polyelectrolyte complexes with negatively charged entities [18]. For example, chitosan interacts with negatively charged DNA and protects it from nuclease degradation, which makes it a good candidate for nonviral gene delivery [19]. Therapeutically, siRNA is used to silence protein activity by blocking the transcription of mRNA to the target protein [20]. However, siRNA has a very low transfection efficiency and is susceptible to degradation before entering target cells [21]. Chitosan nanoparticles have been used effectively to transfect cells with siRNA [22]. *In vitro*, targeting studies of Concanavalin-A (Con-A) immobilized on chitosan nanoparticles were very effective in targeting chemotherapeutic agents to tumor cells and siRNA entrapped in chitosan nanoparticles have good tumor cell uptake [23]. Sood et al. [24] delivered siRNA using chitosan nanoparticles resulting in efficient gene silencing in ovarian carcinoma.

In this study, iron oxide (Fe_3O_4) containing magnetic chitosan nanoparticles were prepared with Con-A and Bleomycin as novel multifunctional nanocarriers for the targeted cancer therapy by co-precipitation techniques. Carrier system, loading with an antineoplastic agent (i.e., Bleomycin, Nippon, Japan) as a model drug and Con-A (*Canavalia ensiformis*, type VI, Sigma, ABD) for targeting, and characterization of morphology, physicochemical characteristics, and magnetic properties of the nanoparticles is described in this section.

MATERIAL AND METHODS

Materials

Ferric chloride hexahydrate ($FeCl_3 \cdot 6H_2O$, 99%), ferrous chloride tetrahydrate ($FeCl_2 \cdot 4H_2O$, 99%), and ammonia (NH_3) (Riedel, Germany) were purchased from Sigma (Taufkirchen, Germany) and ammonia was used as precipitator of ferric salts. Chitosan with different molecular weights (i.e., 150, 450, and 650 kDa, as low molecular weight (LMW), medium molecular weight (MMW), and high molecular weight (HMW), respectively) were obtained from Fluka (Switzerland). Aqueous acetic acid (Carlo Erba, Italy) solutions were used as solvent for the chitosan and sodium triphosphate pentabasic (Sigma Aldrich, ABD) was used as the cross-linker. Water-soluble carbodiimide (WSC) (1-ethyl-3-(3-dimethylaminopropyl) carbodiimide), phosphate buffer, MES buffer (2-(N-morpholino) ethanesulfonic acid, $C_6H_{13}NO_4S$), and glycine, which were purchased from Fluka (Switzerland), were used for Con-A binding studies. Bleomycin, as the model drug, was obtained from Nippon Co., Japan and Con-A (*Canavalia ensiformis*, type VI), from Sigma, ABD. All other chemicals were of reagent grade and used without further purification.

Preparation of Magnetic Fe_3O_4 Nanoparticles

To a solution containing 1.34 g of $FeCl_2 \cdot 4H_2O$ and 3.40 g of $FeCl_3 \cdot 6H_2O$ dissolved in 10 mL of distilled water, 18 mL of 3 M ammonia solution was added slowly with stirring. The color of the suspension immediately turned black, indicating the formation of magnetite. The solution was stirred rapidly for about 1 h at room temperature. The black solution was centrifuged for 30 min at 9000 rpm and the supernatant was used and washed with distilled water several times.

Preparation of Magnetic Chitosan Nanoparticles

Chitosan (0.5 g) was dissolved in 100 mL of 1% acetic acid to form a 0.5% chitosan solution; the pH of the solution was adjusted to 4.8 using 10 M NaOH. To this solution, 1.34 g of $FeCl_2 \cdot 4H_2O$ and 3.40 g of $FeCl_3 \cdot 6H_2O$ were dissolved in 30 mL of 0.5% chitosan solution, 10 mL TPP solution and 18 mL 3 M of ammonia solution were added at the same time. The resulting solution was stirred for 1 h at room temperature. The colloidal magnetic chitosan nanoparticle mixture was centrifuged for 10 min at 9000 rpm. The magnetic and nonmagnetic particles were separated by using a magnet. The obtained magnetic nanoparticles were washed with distilled water several times.

Immobilization of Con-A on Magnetic Chitosan Nanoparticles

Con-A (500 μg/mL) was dissolved in 1 mL of 0.1 M of MES buffer (pH 5.2), mixed with activated 50 mg/mL of magnetic nanoparticles and incubated at 25°C for 24 h on a rotator. The Con-A immobilized magnetic nanoparticles were removed from the medium, washed several times with PBS (0.1 M K_2HPO_4–KH_2PO_4 with pH 7.4) and kept in PBS until use. Coupling efficiencies were determined by measuring the initial and final (before and after immobilization) concentrations of the respective antibodies within the medium using a UV spectrophotometer (Shimadzu, Japan).

Characterization of Nanoparticles

Morphological Evaluations

The morphology of the Fe_3O_4 and Fe_3O_4-loaded chitosan nanoparticles were determined by using a scanning electron microscope (SEM, Jeol, Japan). An aqueous suspension (1.5 mL) of Fe_3O_4 and Fe_3O_4-loaded chitosan nanoparticles were placed on a sample holder in a vacuum at 25°C for 24 h to dry. The samples were coated with gold prior to taking SEM micrographs.

Particle Size, Distribution, and Surface Charge

The average particle size, size distributions, and surface charges of the nanoparticles were determined by Zeta Sizer (Malvern Instruments, Model 3000 HSA, France). In a typical procedure, 2 mL of magnetic chitosan nanoparticle were added to 20 mL of filtered deionized water and sonicated to prevent particle aggregation before the analysis.

Chemical Structure

Fourier transform infrared (FTIR) (Schimadzu, DR8101, Japan) spectroscopy was used to characterize the changes in the chemical structure of Fe_3O_4 nanoparticles after surface stabilization.

Magnetic Properties

Magnetic properties of Fe_3O_4 and Fe_3O_4-loaded chitosan nanoparticles were evaluated with electron spin resonance spectroscopy (ESR) and vibrating sample magnetometer (VSM). ESR measurements were performed at room temperature and spectrometer operating conditions were set as 9.3 GHz, 3300 field set, 100 Hz field modulation, 1 G peak-to-peak modulation amplitude and 1 mW microwave power to determine signal intensities, line widths, and *g*-values. All ESR signal intensities were performed using a standard DPPH sample.

The magnetic properties of the nanoparticles were evaluated by using vibrating-sample magnetometer (LDJ 9600 VSM). A certain amount of Fe_3O_4 nanoparticles and Fe_3O_4-loaded chitosan nanoparticles were used for the analysis. An increasing magnetic field between 0 and 15,000 Oe was applied over the nanoparticles for the determination of the degree of magnetism and the data were used to calculate the magnetic quality of the nanoparticles in electron mass units (emu).

Bleomycin Loading and Release Studies

Dry Fe_3O_4-loaded chitosan nanoparticles (50 mg) were pre-swollen in 1 mg solutions containing different concentrations of Bleomycin (1, 3, 5 mg/mL) and incubated about 15 h with constant shaking, The ensuing mixture was centrifuged at 15,000 rpm to separate the nanoparticles that were used for release studies. For another part of these studies, different molecular weights of chitosan were used to prepare Bleomycin loaded nanoparticles and 5 mg/mL of Bleomycin was used in all of the samples. To determine the Bleomycin loading and release rates, calibration curves were prepared by dissolving 1 mg of Bleomycin in phosphate buffer (pH 7.2) and then diluted to 2, 4, 8, 16 μg/mL. The absorbances were obtained by using a UV spectrometer (Mini UV 1240, Schimadzu, Japan) at 291 nm, to establish a standard curve; these studies were carried out at $37 \pm 1^{\circ}C$ and pH 7.2 ± 0.4. In the *in vitro* release studies, 10 mL of phosphate buffer solution was put into two cells separated by a dialysis membrane and 50 mg of chitosan nanoparticles including specific amounts of Bleomycin were added into one of the cells. At 25-min intervals, 100 μL of solution containing released Bleomycin was taken from the cell that contained no nanoparticles and the amount of the drug was measured by UV spectrometer.

Cytotoxicity Assay (MTT)

HeLa cells were cultured in DMEM-F12 medium supplemented with 10% FCS and 1% antibiotics (100 units of penicillin and 100 mg streptomycin) in a humidified incubator at 37°C and in 5% CO_2 atmosphere. The cells were sub-cultured twice a week, using a dissociation medium, Trypsin-EDTA, pH 7.4 as buffer system [25]. The MTT (3-[4,5-dimethylthiazol-2-yl]-2,5-diphenyltetrazoluim bromide and thiazolyl blue) assay is an assay to measure cell viability. The cytotoxicity effects of magnetic chitosan nanoparticle, magnetic chitosan nanoparticle-Con-A, Bleomycin loaded magnetic chitosan nanoparticle, and Bleomycin loaded magnetic chitosan nanoparticle-Con-A were investigated on cultured HeLa cells. Cells were plated in 96-well culture plates with 10×10^3 cell/well and cultured with DMEM-F12 supplemented with 10 % fetal bovine serum (FBS) and 1% penicillin–streptomycin antibiotic humidified under 5% CO_2 at 37°C for 24 h. The nanoparticles were diluted with the cell culture medium and inoculated to the cells and incubated for another 24 h. After the incubation, medium was removed and 100 μL fresh medium and 13 μL MTT solution (5μg/mL, diluted with RPMI 1640 without phenol red) were added to each well and allowed incubation for another 4 h in dark medium at 37°C. Since living cells metabolize the MTT in their mitochondria and form blue formazan crystals, 100 μL/well isopropanol–HCl (absolute isopropanol containing 0.04 M HCl) solution was added to dissolve the formazan crystals. The wells were read at 570 nm on an ELISA plate reader and the percentage of viability was calculated. For each MTT assay, the control HeLa cell viability was defined as 100 % [26].

RESULTS AND DISCUSSION

Morphological Evaluations

The immobilization of Con-A onto the magnetic nanoparticles, a well-known protocol, was used, as shown in Figure 1 [27]. Micrographs of Fe_3O_4 and Fe_3O_4-loaded chitosan nanoparticles are shown in Figures 2 and 3, respectively. The magnetic Fe_3O_4 nanoparticles were well-shaped spheres ~50 nm in diameter. The Fe_3O_4-loaded chitosan nanoparticles were also spherical but larger in size (~150 nm).

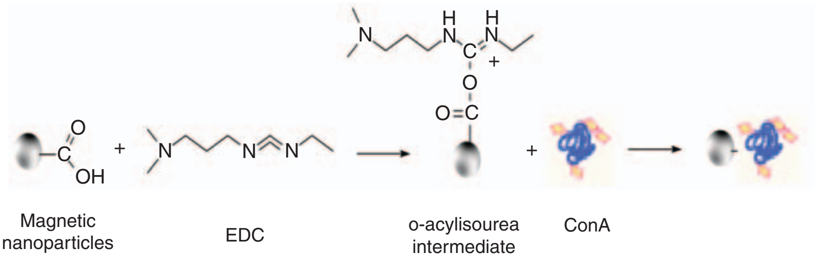

Figure 1. Con-A binding mechanism onto the magnetic chitosan nanoparticles.

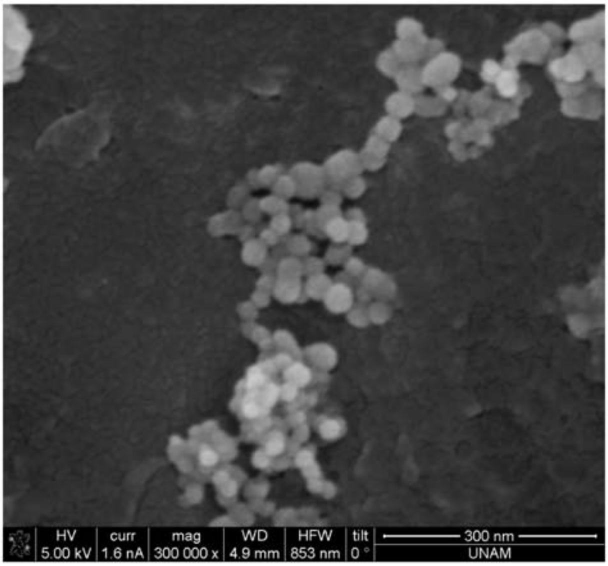

Figure 2. SEM micrograph of Fe_3O_4 nanoparticles.

Size and Size Distributions of Fe_3O_4 Nanoparticles

The particle sizes, averaged from 30 measurements and the size distributions (PDI) recorded automatically by the software, are summarized in Tables 1 and 2 for Fe_3O_4 and Fe_3O_4-loaded chitosan nanoparticles, respectively. The Fe^{2+}/Fe^{3+} ratio was one of the parameters that affected the particle size of Fe_3O_4 nanoparticles produced by the precipitation method [19]. However, it was not possible to produce stable magnetite latexes with a ratios lower than 0.5 Fe^{2+}/Fe^{3+}. When we increased the relative concentration of Fe^{2+} ions in the solution, the particle sizes were larger and the particle size distribution

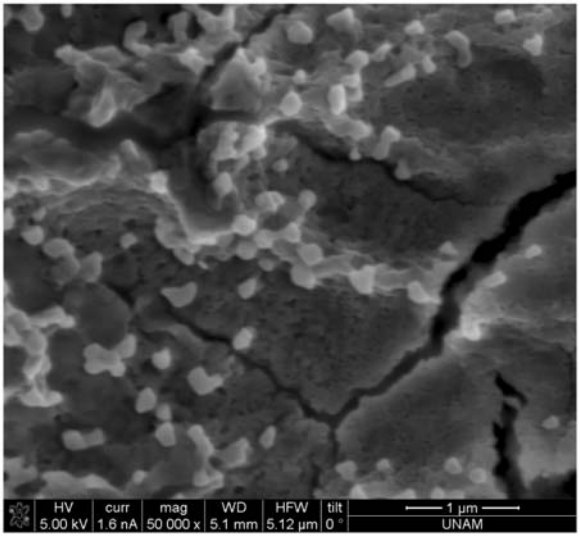

Figure 3. SEM micrograph of Fe_3O_4-loaded chitosan nanoparticles.

Table 1. Effective parameters on size-size distribution of the Fe_3O_4 nanoparticles.

Sample no.	Fe^{2+}/Fe^{3+} mole ratio	Stirring rate (rpm)	Size (nm)
Effects of Fe^{2+}/Fe^{3+} mole ratio			
1	0.5	2000	22.25 ± 2.50
2	1.0	2000	31.25 ± 2.63
3	1.5	2000	73.50 ± 3.11
4	2.0	2000	125.00 ± 2.16
Effects of stirring rate			
5	0.5	1000	285.00 ± 6.70
6	0.5	1250	176.75 ± 4.65
7	0.5	1500	107.50 ± 2.08
8	0.5	2000	22.25 ± 2.50

broader due to the oxidative instability of Fe^{+2} ions in the medium as related in the studies [28,29].

The stirring rate dispersed the suspension of Fe_3O_4 and Fe_3O_4-loaded chitosan nanoparticles into droplets and higher stirring rates produced smaller nanoparticles and narrower size distributions [30]. In this study, the particle size was decreased significantly from 285 to 22 nm, respectively, by increasing the rate from 1000 to 2000 rpm. The narrowest particle size distribution was also observed at 2000 rpm.

Table 2. Effective parameters on size-size distribution of the Fe_3O_4-loaded chitosan nanoparticles.

Sample no.	Chitosan MW	Chitosan/TPP weight ratio	Size (nm)
Effects of chitosan MW			
1	LMW (150 kDa)	0.5	156.67 ± 5.86
2	MMW (450 kDa)	0.5	260.33 ± 8.33
3	HMW (650 kDa)	0.5	309.67 ± 10.53
Effects of chitosan/TPP weight ratio			
5	LMW (150 kDa)	0.5	156.67 ± 5.86
7	LMW (150 kDa)	1.0	371.33 ± 20.13
8	LMW (150 kDa)	1.5	430.00 ± 18.19

The size of the nanoparticles was increased by increasing the molecular weight of chitosan. With the longer molecular chain lengths, there is a higher possibility of crosslinking with TPP to produce larger sized nanoparticles. The nanoparticle size increased linearly with increasing chitosan to TPP weight ratio. The linear relationship provides a simple processing window for manipulating and optimizing the nano size for intended applications.

Chemical Structure

For the FTIR spectra of the naked Fe_3O_4 and Fe_3O_4, the peaks at 673 and 408 cm^{-1} were related to the Fe–O group. The peak at $\sim$3455 cm^{-1} for chitosan and Fe_3O_4-loaded chitosan nanoparticles related to the – OH group. The IR spectrum of chitosan nanoparticles had characteristic absorption bands at 1598 cm^{-1}, that were assigned to N–H bending vibration, and peaks at 1220 cm^{-1} to C–O stretching and at 1620 cm^{-1} to C=O stretching. In the spectrum of Fe_3O_4-loaded chitosan nanoparticles, compared with the spectrum of chitosan nanoparticles, the 1598 cm^{-1} peak of N–H bending vibration; a new sharp peak at 670 cm^{-1} related to Fe–O group, specific for the stretching vibration of Fe–O groups from the magnetite nanoparticles, confirmed the loading of the Fe_3O_4 on chitosan [31–33].

Magnetic Properties

The ESR data for Fe_3O_4 and Fe_3O_4-loaded chitosan nanoparticles are given in Table 3. The magnetite particles typically showed intensity at an applied magnetic field of $\sim$3975 G while the relative intensity of the Fe_3O_4-loaded chitosan nanoparticles was $\sim$3650 G. The shift was attributed to the polymer on the surface of the nanoparticles.

Table 3. ESR data for Fe_3O_4 nanoparticles and Fe_3O_4-loaded chitosan nanoparticles.

Sample	Size (nm)	*g*	ΔH_{pp}	*Hr*
Fe_3O_4 nanopartices	22	1.9978	1410	3975
Fe_3O_4-loaded chitosan nanoparticles	180	1.8915	1378	3650

The magnetic properties of magnetic polymeric particles were also studied by using a vibrating-sample magnetometer. Here, the applied magnetic field (Oe) was changed and magnetization (M, emu/g) was measured. Both, the Fe_3O_4 nanoparticles and Fe_3O_4-loaded chitosan nanoparticles, were super-paramagnetic and no remanence was observed when the magnetic field was removed. The saturation magnetizations obtained for Fe_3O_4 nanoparticles and Fe_3O_4-loaded chitosan nanoparticles were 5.6 and 1.25 emu/g, respectively. The decrease in the saturation magnetization was due to the increased amount of polymer incorporated in the polymer-coated magnetite suspension.

In vitro Release of Bleomycin from Magnetic Chitosan Nanoparticles

Bleomycin concentration was used as an effective parameter to evaluate further optimization studies [10]. The nanoparticles were incubated with different concentrations of Bleomycin solutions (1, 3, 5 mg/mL); the release was significantly greater in initial stage for all of the formulations. This burst effect is normally seen as the most of the Bleomycin was near the surface of the nanoparticles. In addition, higher release rates also occur from higher lading ratios.

In the *in vitro* release studies, different chitosan molecular weights were used to enhance the loading of Bleomycin in the chitosan nanoparticles. The Bleomycin release rates were very similar for all of the formulations with different molecular weights of chitosan (Figure 4). The Bleomycin release was increased by increasing the molecular weight of chitosan. This can be explained by the presence of the longer polymer chains with more active sights for the attachment of Bleomycin. This lead to the increase in loading and release ratios of Bleomycin with chitosan molecular weight.

Cytotoxicity Assay (MTT)

The *in vitro* cytotoxicity of the nanoparticles was measured as a function of nanoparticle composition and concentration using the MTT

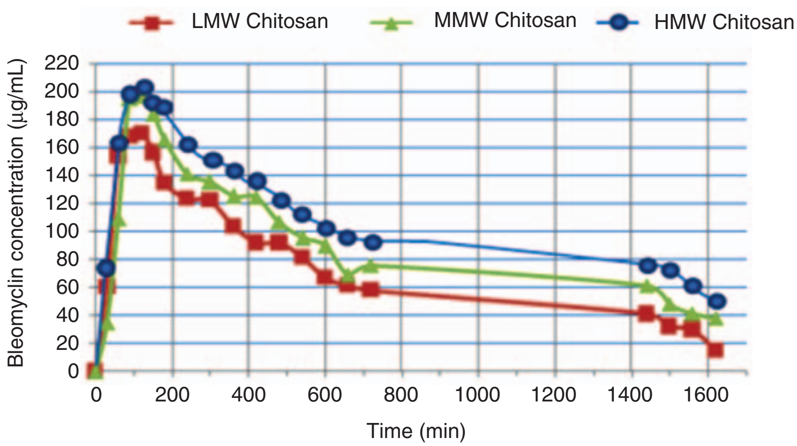

Figure 4. Effects of chitosan molecular weight over the Bleomycin release rates.

Table 4. MTT results for magnetic chitosan nanoparticles with different formulations.

	Nanoparticle concentration (µg/mL)	Cell viability (%)
	0 (Control)	100 ± 0.05
Free forms	Bleomycin*	73.1 ± 0.98
	Con-A*	86.3 ± 0.51
Magnetic chitosan nanoparticle	10	76.7 ± 0.92
	50	64.8 ± 0.05
	100	64 ± 0.65
Magnetic chitosan nanoparticle-Con-A	10	62.6 ± 0.10
	50	39.3 ± 0.46
	100	21.4 ± 0.56
Magnetic chitosan nanoparticle – Bleomycin	10	67.3 ± 0.10
	50	61.4 ± 0.28
	100	53.5 ± 0.80
Magnetic chitosan nanoparticle – Bleomycin–Con-A	10	6.6 ± 0.66
	50	45 ± 0.46
	100	43.1 ± 0.87

*Free Bleomycin and Con-A were used as control and the concentrations were calculated based on the 100 µg/mL of magnetic chitosan nanoparticle Bleomycin and Con-A contents.

assay as reported in Table 4. In the case of magnetic chitosan nanoparticles alone with HeLa cells the cell viability was higher than the other formulations. The magnetic chitosan nanoparticles were nontoxic in terms of biocompatiblity. The cytotoxic effect increased by increasing the nanoparticle concentration in almost every case except the Bleomycin loaded and Con-A attached to magnetic chitosan nanoparticles. It is well known that both iron oxide and Con-A have some cytotoxicity [34], therefore this was expected. Cell viability was slightly increased by increasing the concentration for Bleomycin loaded and Con-A attached to the nanoparticles. This is probably due to the nanoparticle aggregation above certain concentration of nanoparticles (>100 μg/mL). The effects of Bleomycin and Con-A alone were evaluated with free Bleomycin and Con-A as control groups. The effects of the Bleomycin and Con-A increased when combined with the chitosan nanoparticles. This is an expected result as magnetic chitosan nanoparticles have certain toxicity for 100 μg/mL concentration without any drug or ligand as seen in Table 4.

CONCLUSIONS

Nanoparticles and magnetic chitosan nanoparticles were prepared by chemical methods using precipitation and co-precipitation techniques. The sizes ranged from 15 to 180 nm for the iron oxide nanoparticles and 150 to 430 nm for the magnetic chitosan nanoparticles. The magnetic characteristics of the nanoparticles was not altered significantly in the case of magnetic chitosan nanoparticles compared to the iron oxide nanoparticles. Bleomycin was loaded onto the magnetic chitosan nanoparticles and the model ligand, Con-A, was attached after the formation of nanoparticles. The release profile of Bleomycin was readily adjusted by changing the preparation conditions. The effectiveness of Bleomycin loaded magnetic chitosan nanoparticles were evaluated by cytotoxicity tests and nanoparticles–cell interaction studies. These Bleomycin and Con-A magnetic chitosan nanoparticles are promising for cancer therapy as a new smart nanotherapeutic system.

REFERENCES

1. Stewart, B.W. and Kleihues, P. (eds) (2003). *World Cancer Report*, Lyon: IARC Press.
2. Alison, M.R. (2003). *The Cancer Handbook*, London: Nature Publishing Group.
3. Bertino, J. (2002). *Four-Volume Set, 1–4*, London: Academic Press.
4. Catane, R., Cherny, N.I., Kloke, M., Tanneberger, S. and Schrijvers, D. (2006). *Handbook of Advanced Cancer Care*, Oxford: Taylor & Francis.
5. Gabriel, J. (2007). *The Biology of Cancer*, New York: John Wiley & Sons.
6. Llombart, A., Felipo, V. and Lopez-Guerrero, J.A. (eds) (2006). *New Trends in Cancer for the 21st Century*, New York: Springer.

7. Jain, R.K. (2001). Delivery of Molecular and Cellular Medicine to Solid Tumors, *Advanced Drug Delivery Reviews*, **46**: 149–168.
8. Parmiani, G., Castelli, C., Dalerba, P., Mortarini, R., Rivoltini, L., Marincola, F.M. et al. (2002). Cancer Immunotherapy with Peptide-based Vaccines: What have We Achieved? - Where are We Going?, *Journal of the National Cancer Institute*, **94**: 805–818.
9. Jang, S.H., Wientjes, M.G., Lu, D. and Au, J.L.S. (2003). Drug Delivery and Transport to Solid Tumors, *Pharmaceutical Research*, **20**: 1337–1350.
10. Guowei, D., Adriane, K., Chen, X.Z., Jie, C. and Yinfeng, L. (2007). PVP Magnetic Nanospheres: Biocompatibility, In Vitro and In Vivo Bleomycin Release, *International Journal of Pharmaceutics*, **328**: 78–85.
11. Bentzen, S.M. (2005). Theragnostic Imaging for Radiation Oncology: Dose-painting by Numbers, *Lancet Oncol*, **6**: 112–117.
12. Neuberger, T., Schöpf, B., Hofmann, H., Hofmann, M. and von Rechenberg, B. (2005). Superparamagnetic Nanoparticles for Biomedical Applications: Possibilities and Limitations of a New Drug Delivery System, *Journal of Magnetism and Magnetic Materials*, **293**: 483–496.
13. Jordan, A., Wust, P. Scholz, R., Faehling, H., Krause, J. and Felix, R. (1997). Magnetic Fluid Hyperthermia, In: Haneli, U., Schütt, W., Teller, J. and Zborowski, M. (eds), *Scientific and Clinical Applications of Magnetic Carriers*, p. 569, New York: Plenum Press.
14. Kim, D.H., Lee, S.H., Im, K.H., Kim, K.N., Kim, K.M., Shim, I.B. et al. (2006). Surface-modified Magnetite Nanoparticles for Hyperthermia: Preparation, Characterization, and Cytotoxicity Studies, *Current Applied Physics*, **6S1**: e242–e246.
15. Gupta, A.K. and Gupta, M. (2005). Synthesis and Surface Engineering of Iron Oxide Nanoparticles for Biomedical Applications, *Biomaterials*, **26**: 3995–4021.
16. Denkbaş, E.B. and Ottenbrite, R.M. (2006). Perspectives on: Chitosan Drug Delivery Systems: Based on their Geometries, *Journal of Bioactive and Compatible Polymers*, **21**: 351–368.
17. Rinaudo, M. (2006). Chitin and Chitosan: Properties and Applications, *Progress in Polymer Science*, **31**: 603–632.
18. Majeti, N.V. and Kumar, R. (2000). A Review of Chitin and Chitosan Applications, *Reactive & Functional Polymers*, **46**: 1–27.
19. Dang, J.M. and Leong, K.W. (2006). Natural Polymers for Gene Delivery and Tissue Engineering, *Advanced Drug Delivery Reviews*, **58**: 487–499.
20. Rozema, D.B. and Lewis, D.L. (2003). siRNA Delivery Technologies for Mammalian Systems, *Targets*, **2**: 253–260.
21. Aigner, A. (2006). Gene Silencing Through RNA İnterference (RNAi) İn Vivo: Strategies Based on the Direct Application of siRNAs, *Journal of Biotechnology*, **124**: 12–25.

22. Katas, H. and Alpar, H.O. (2006). Development and Characterisation of Chitosan Nanoparticles for siRNA Delivery, *Journal of Controlled Release*, **115**: 216–225.

23. Ozturk, E. (2007). Preparation and Characterization of Biochemically Modified Polymeric Carriers for Cancer Therapy, Thesis, Hacettepe University.

24. Sood, A.K., Mangala, L.S., Han, H., Lu, C., Ali-Fehmi, R., Stone, R. et al. (2009). In Vivo Angiogenic Gene Silencing Using Chitosan Nanoparticles in Ovarian Carcinoma, *Gynecologic Oncology*, **112**: 136–137.

25. Marques, M.P.M., Girao, T., De Lima, M.C.P., Gameiro, A., Pereira, E. and Garcia, P. (2002). Cytotoxic Effects of Metal Complexes of Biogenic Polyamines. I. Platinum (II) Spermidine Compounds: Prediction of their Antitumor Activity, *Biochimica et Biophysica Acta*, **1589**: 63–70.

26. Demirbilek, M. and Pişkin, E. (2008). Effects of Copper-Cyclam and Copper-Cyclam/Polymer Complexes on HeLa Cells, *Hacettepe Journal of Biology & Chemistry*, **36**: 263–271.

27. Bangs Laboratories (2002). Technotes 205, Rev 003, pp. 1–8.

28. Zhu, Y. and Wu, Q. (1999). Synthesis of Magnetite Nanoparticles by Precipitation with Forced Mixing, *Journal of Nanoparticle Research*, **1**: 393–396.

29. Pardoe, H., Chua-Anusorn, W., St. Pierre, T.G. and Dobson, J. (2001). Structural and Magnetic Properties of Nanoscale Iron Oxide Particles Synthesized in the Presence of Dextran or Polyvinyl Alcohol, *Journal of Magnetism and Magnetical Materials*, **225**: 41–46.

30. Denkbaş, E.B. and Odabaşı, M. (2000). Chitosan Microspheres and Sponge: Preparation and Characterization, *Journal of Applied Polymer Science*, **76**: 1673–1643.

31. Yamaura, M., Camilo, R.L., Sampao, L.C., Macedo, M.A., Nakamura, M. and Toma, H.E. (2004). Preparation and Characterization of (3-Aminopropyl)Triethoxysilane-Coated Magnetite Nanoparticles, *Journal of Magnetism and Magnetical Materials*, **279**: 210–217.

32. Sayar, F., Güven, G. and Pişkin, E. (2006). Magnetically Loaded Poly(Methyl Methacrylate-Co-Acrylic Acid) Nano-particles, *Colloidal Polymer Science*, **284**: 965–978.

33. Li, G., Jiang, Y., Huang, K.L., Ding, P. and Chen, J. (2008). Preparatıon and Propertıes of Magnetıc Fe_3O_4-Chıtosan Nanopartıcles, *Journal of Alloys and Compounds*, **466**: 451–456.

34. Delfini, C., Amici, C., Belardelli, F., Oberholtzer, G. and Sorrentino, M. (1982). Concanavalin A-induced İnhibition of Abrin and Ricin Activity Parallels with a Decrease of the Number of Toxin-binding Uptake-elution Cycles, *Experimental Cell Research*, **142**: 427–435.